Mechanical energy analysis of a boomerang mechanism

C. Álvarez-Macías^a, L. Salgado-Conrado^b, J. De la Cruz-Canul^a and M. Rivero^c

^{a}*Tecnológico Nacional de México/Instituto Tecnológico de La Laguna.*
27000, Torreón, Coahuila, México.
^{b} *Facultad de Ingeniería Mecánica y Eléctrica, Universidad Autónoma de Coahuila,*
Carr. Torreón-Matamoros, km 7.5, 27276, Torreón, Coahuila, Mexico.
^{c} *CONACYT - Instituto Tecnológico de La Laguna. 27000, Torreón, Coahuila, México.*

In this paper, we present a comparison of classical theory with video analysis techniques to teach kinetic and potential energy of a device with a boomerang effect as an observable and measurable concept. The device can store energy through an elastic band when it rolls down an inclined plane, and can release the energy when it rolls on a horizontal surface; hence, it receives the name boomerang. In theoretical terms, the details of energy charge and discharge processes are analyzed with Newton's laws and Lagrangian method. The experimental results were recorded with cell phone cameras and processed with an open-source video analysis software, called "Tracker". The comparison shows relevant concepts about kinetic and potential energy, which can help the student to overcome some of the typical student misconceptions.

Keywords: Boomerang; energy conservation; Lagrange equations; Newton's laws; harmonic movement.

En este artículo, presentamos una comparación de la teoría clásica con técnicas de análisis de video para enseñar la energía cinética y potencial de un dispositivo con un efecto búmeran, como un concepto observable y medible. El dispositivo puede almacenar energía a través de una banda elástica cuando rueda hacia abajo en un plano inclinado y puede liberar la energía cuando rueda sobre una superficie horizontal; de ahí el nombre de búmeran. En términos teóricos, los detalles de los procesos de carga y descarga de energía se analizan con las leyes de Newton y el método de Lagrangian. Los resultados experimentales se registraron con cámaras de teléfonos celulares y se procesaron con un software de análisis de video de código abierto, llamado "Tracker". La comparación muestra conceptos relevantes sobre la energía cinética y potencial, que pueden ayudar al estudiante a superar algunos de los conceptos erróneos típicos de los estudiantes.

Descriptores: Búmeran; conservación de la energía; ecuaciones de Lagrange; leyes de Newton; movimiento armónico.

PACS: 01.50.My, Wg; 02.30.Hq; 01.55.+b; 06.30.Gv; 45.20.Jj; 45.20.dc; 45.40.Cc; 88.05.-b

DOI: https://doi.org/10.31349/RevMexFisE.17.19

1. Introduction

The mechanical energy conservation has gained so much attention due to this issue occupies a central place in physics instruction at all levels. This concept is traditionally associated with different subjects with several engineering activities. Although energy conservation is a classical problem in physics, the understanding students in this topic is unsatisfactory and limited. It is often because when the student examines the literature, different misconceptions about the concept of energy emerges.

Various research in science education studied and proposed solution about the difficulties of students in understanding the concept of energy and in using its conservation principle in practical examples. For example, Takaoglu [1] determined how high school students at different levels perceive the energy and related concepts. The results showed that energy and associated concepts are disconnected in different lessons of different disciplines, so that, the students do not relate concepts.

İYİBİL [2] determined the effectiveness of the teaching "energy" concept based on the Common Knowledge Construction Model. The result of this study shows that the lessons' time in the science curriculum is not enough, especially, if students have learning difficulties. They concluded that it is more successful to teach a concept or a subject in controlled groups than individually. Tatar [3] studied published manuscripts on students' misunderstandings about the energy conservation principle with the purpose to prevent these misunderstandings. The authors gave some crucial strategies to reduce or eliminate misunderstandings on the energy conservation principle.

Heuvelen and Zou [4] described a multiple-representation strategy for helping students to analyze work-energy processes along with several examples. The results showed that the qualitative work-energy bar charts served as a useful visual tool to help students understand work-energy concepts and to solve related problems.

Tiberghien [5] presented the methodology to teach the energy concepts at the high school level. The method is based on relating the theory and the model (in a written form) with the experimental field (in the way of a real experiment). According to results, the combination permits the construction of coherent relations between these two worlds.

Liu *et al*. [6] examined the structural characteristics of university engineering students' conceptions of energy conservation. It was found that students failed to apply the concepts of energy conservation in practical examples. Therefore, it has serious implications for science curriculum development and instruction.

For this perspective, the primary challenge is to introduce new practical examples, where the student incorporates classical theory with software analysis techniques. Therefore, in this paper, a comparison of classical theory with a video analysis technique is used to teach kinetic and potential energy of a device with a boomerang effect. The mathematical model is based on Lagrange's equations and Newton's laws. The experimental results were recorded with cell phone cameras and processed with an open-source video analysis software, called 'Tracker'.

Our efforts aimed to show the student the relationship between the kinetic and potential energy of a mechanical device with a boomerang effect, the influence of the elastic band when the mechanic is rolling on an inclined plane without slipping, and total mechanical energy of the studied object.

The remainder of the paper is organized as follows. Section 2 introduces the methodology. Section 3 describes background information from the literature about relevant factors. Section 4 describes in detail the operational principle of the mechanical device with a boomerang effect. Section 5 presents the dynamic equations using the Lagrangian method and Newton's laws. Section 6, discusses the experimental and mathematical results. Finally, in Sec. 6, we give concluding remarks.

2. Methodology

The analytical and experimental comparison follows the next procedure: i) introduction to related literature, ii) description of mechanical device, iii) construction of the mathematical model, iv) obtaining and comparing the experimental and theoretical data; and v) check that the correlation of the data is correct.

3. Related literature

The boomerang effect is a particularly important, intriguing and widely known case of bodies in rotation. Its peculiar characteristic is to rotate throughout a trajectory and return to their point of origin, due to the rotational inertia of the body [7]. The boomerang effect has been studied from the aerodynamic point of view by [8–10]. In change, the mechanical devices subject to rolling on a horizontal plane is one of the most studied problems in physics, due to its applicability in ball bearing, moving vehicles and tribology [11].

Many research works have examined the rolling from several points of view. For example, Yavin and Frangos [12] introduced the concept of available command strategies and their applicability onto a disk rolling on a moving horizontal plane. The significant findings of their work are; i) to find the equations of motion of the disk using the Lagrangian method during a time interval $[0, t_f]$, and ii) using open-loop strategies to compute the results. In other work [13], the authors analyzed a disk rolling on a vibrating plane. There, they introduced the concept of path controllability model to demonstrate its applicability. The dynamic model offers a procedure

for the design of closed-loop control law applicable in disk's motion with path controllable.

Kemp and Yavin [14] have developed a procedure for the calculation of torques in disk's motion, which allows tracking and gives a smooth ground trajectory. This work explored the possibility of controlling the motion of the rolling disk by applying two rotors. Cushman and Duistermaat [15] analyzed the motion and loss of energy of a disk without slipping. Lagrangian equations and Newton's laws were used to define the position, velocity, and energy of a thin disk. In [16], the second-year undergraduate studies used computer algebra as a tool to analyze the conservation of energy, the position of the centroid and the stability of a disk on a horizontal plane. The experiments based on video analysis indicate that students' understanding improved remarkably and some typical difficulties were overcome.

In Maloney [17], the author investigated the energy transformations about five situations involving the conservation of mechanical energy, using Siegler's Rule-Assessment technique. In each case, the study showed the relation between conceptual and experimental analysis and identified several strategies to connect the terminology.

Batista *et al*. [18] provided a discussion about steady motion of a rigid disk with finite thickness rolling on its edge, on a horizontal plane under the influence of gravity. The authors included a complete study of the bifurcations of steady motion on rough ground. Similarly, in [19], the author provided a solution to the bifurcations of the steady motion of a disk on a rough plane, using Gauss hypergeometric functions. In [20, 21], the displacement, speed, and acceleration of a disk on an inclined plane without slipping were analyzed using the Lagrangian method.

In this paper, a video analysis technique is used to help relate concepts through the visual tool. The proposed technique was the students' validation in a test-bed, with theory frame of energy conservation, through visual tools, they linked the theory with practical experiments. It was noticed that this method could reduce some misunderstandings on the energy conservation principle.
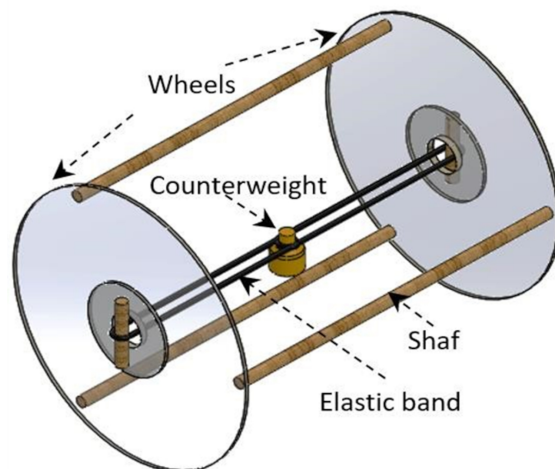
FIGURE 1. Schematic of the BW mechanism.

4. System description

Figure 1 shows a CAD model of a boomerang wheel (BW) mechanism. The mechanical system has a structure in a cylindrical shape. It is composed of two lateral wheels with radius (r_w) joined to three longitudinal shafts. The shafts are distributed around the wheels at $120°$ and located at a radius (r_p) from the center to the periphery. Each shaft has a length (L_s) and diameter (r_s).

The BW mechanism includes an elastic band traversed by the central axis of the structure and fixed at its end wheels. At the middle of the elastic band, a counterweight is tied in such a way that the wheels rotate without the counterweight moving.

The mechanical system is placed at the top of a ramp at a height (h) of 0.13 m. In this position (P_1), the wheels remain static with a brake. When the BW mechanism releases from rest, it moves down the ramp (P_2). During the movement, the elastic band begins to turn. The torsion of the elastic band will cause the wheels to slow down and the mechanism to stop (P_3). In this phase, the mechanism is in the process of charging energy. Figure 2 illustrates the trajectory of the BW mechanism.

When the elastic band is completely twisted (P_3), the BW mechanism begins to move in a contrary sense (the boomerang effect), from P_3 to P_2, from P_2 to P_3, and so on. The mechanism repeats the charge and discharge process until it stops, dissipating all the energy of the elastic band. In this phase, the system is in the process of discharging energy.

5. Mathematical formulation

5.1. Process of charging energy

The BW mechanism will be considered a solid disk of radius r_w and mass m_w, that starts from rest and travels without sliding up a slope with an opening angle ϕ. The reference system xy is located at the top of the ramp, as indicated in Fig. 3. When the mechanism moves from P_1 to P_2, the potential energy V is expressed by [22]

$$V = m_T g y_G + \frac{1}{2} k_t \theta^2 \qquad (1)$$

where $k_t = \omega_n^2 I_T$.
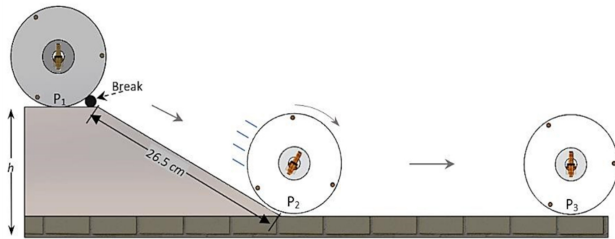
FIGURE 2. Trajectory of the BW mechanism.
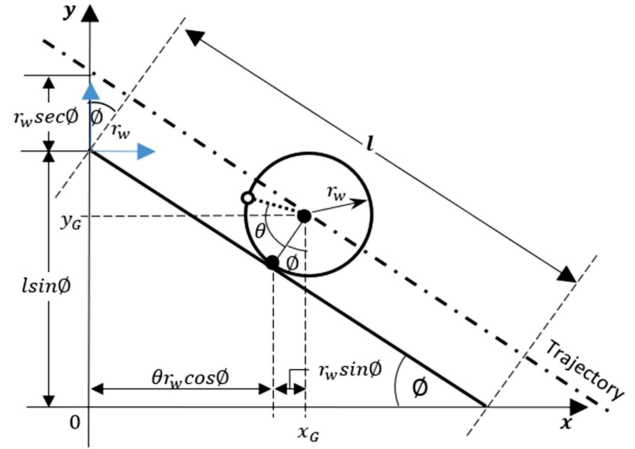
FIGURE 3. Free body diagram of the BW mechanism.

The kinetic energy is given by the sum of translation and rotation motion around the centre of mass, as Eq. (2) shows [23]:

$$T = \frac{1}{2} m_T (\dot{x_G}^2 + \dot{y_G}^2) + \frac{1}{2} I_T \dot{\theta}^2 \qquad (2)$$

where $I_T = m_w r_w^2 + m_s r_p^2$, $I_w = m_w r_w^2$, and $I_s = m_s r_p^2$.

Therefore, the total energy of the system is expressed as

$$E_T = \frac{1}{2} m_T (\dot{x_G}^2 + \dot{y_G}^2) + \frac{1}{2} I_T \dot{\theta}^2 + m_T g y_G + \frac{1}{2} k_t \theta^2. \qquad (3)$$

The Lagrangian method [24] is applied to obtain the equations of motion of the disk rolling on an inclined plane. The Lagrangian function for the system's motion is given by

$$L = T - V = \frac{1}{2} m_T (\dot{x_G}^2 + \dot{y_G}^2)$$
$$+ \frac{1}{2} I_T \dot{\theta}^2 - m_T g y_G - \frac{1}{2} k_t \theta^2 \qquad (4)$$

From Fig. 3, we consider the following holonomic ligatures

$$f_1^{(h)} = (x_G - r_w \sin \phi) \sec \phi - r_w \theta = 0 \qquad (5)$$

$$f_2^{(h)} = y_G + x_G \tan \phi - l \sin \phi - r_w \sec \phi = 0 \qquad (6)$$

The three equation of motion with respect to x_G, y_G and θ, respectively, are

$$m_T \ddot{x_G} = \lambda_1 \sec \phi + \lambda_2 \tan \phi \qquad (7)$$

$$m_T \ddot{y_G} + m_T g = \lambda_2 \qquad (8)$$

$$I_T \ddot{\theta} + k_t \theta = -\lambda_1 r_w \qquad (9)$$

Combining the holonomic ligatures with the three equations of motion and harmonic movement $x_G = A \cos(\omega_n t)$, we obtain

$$\ddot{x_G} = \frac{r_w^2 m_T g \tan \phi - k_t \sec^2 \phi (A \sin(\omega_n t) - r_w \sin \phi)}{m_T r_w^2 - I_T \sec^2 \phi + m_T r_w^2 \tan^2 \phi} \qquad (10)$$

Integrating Eq. (10) with initial conditions $t_0 = 0$, $x_{G_0} = 0$, $\theta_0 = 0$, and $\dot{\theta}_0 = 0$, we have

$$\dot{x_G} = \frac{tD \tan \phi + E\omega_n^{-1} \cos (\omega_n t) + tF}{m_T r_w^2 - I_T \sec^2 \phi + m_T r_w^2 \tan^2 \phi} \tag{11}$$

$$x_G = \frac{0.5t^2 D \tan \phi + \omega_n^{-2} E \sin (\omega_n t) + 0.5t^2 F}{m_T r_w^2 - I_T \sec^2 \phi + m_T r_w^2 \tan^2 \phi} \tag{12}$$

Where $D = r_w^2 m_T g$, $E = k_t A \sec^2 \phi$ and $F = r_w k_t \sin \phi \sec^2 \phi$.

Therefore, the total energy of the BW mechanism for the charge process from P_1 to P_2 can be expressed as

$$E_T(t) = \frac{1}{2}m_T \left(\frac{tD \tan \phi + E\omega_n^{-1} \cos (\omega_n t) + tF}{m_T r_w^2 - I_T \sec^2 \phi + m_T r_w^2 \tan^2 \phi} \right)^2 + \frac{1}{2}m_T \tan^2 \phi \left(\frac{tD \tan \phi + \omega_n^{-1} E \cos (\omega_n t) + tF}{m_T r_w^2 - I_T \sec^2 \phi + m_T r_w^2 \tan^2 \phi} \right)^2$$

$$+ \frac{I_T}{2r_w^2} \left(\frac{tD \tan \phi + \omega_n^{-1} E \cos (\omega_n t) + tF}{m_T r_w^2 - I_T \sec^2 \phi + m_T r_w^2 \tan^2 \phi} \right)^2 - W_T \tan \phi \left(\frac{0.5t^2 D \tan \phi + \omega_n^{-2} E \sin (\omega_n t) + 0.5t^2 F}{m_T r_w^2 - I_T \sec^2 \phi + m_T r_w^2 \tan^2 \phi} \right)$$

$$+ W_T l \sin \phi + W_T r_w \sec \phi + \frac{k_t}{2r_w^2} \left(\frac{0.5t^2 D \tan \phi + \omega_n^{-2} E \sin (\omega_n t) + 0.5t^2 F}{m_T r_w^2 - I_T \sec^2 \phi + m_T r_w^2 \tan^2 \phi} \right)^2 \tag{13}$$

Where W_T is total weight of boomerang mechanism.

The Lagrangian of the disk rolling without slipping from P_2 to P_3 is given by

$$L = T - V = \frac{1}{2}m_T \dot{x_G}^2 + \frac{1}{2}I_T \dot{\theta}^2 - \frac{1}{2}k_t \theta^2 \tag{14}$$

Considering the holonomic ligature $f_1^{(h)} = x_G - r_w \theta = 0$, we obtain the motion equations with respect to x_G and θ, respectively, as follows

$$m_T \ddot{x_G} = \lambda_1 \tag{15}$$

$$I_T \ddot{\theta} + k_t \theta = -\lambda_1 r_w \tag{16}$$

The movement is simple harmonic motion, so $x_G = A \cos (\omega_n t)$, $\dot{x_G} = -A\omega_n \sin (\omega_n t)$, and $\ddot{x_G} = -\omega_n^2 A \cos (\omega_n t)$. Combining these expressions with Eq. (15) and Eq. (16), we obtain $\ddot{x_G} = (-k_t A \cos(\omega_n t)/m_T r_w^2 + I_T)$. Therefore, the total energy of the BW device from P_2 to P_3 can be expressed as

$$E(t) = \frac{1}{2}m_T A^2 \omega_n^2 \sin^2 (\omega_n t) + \frac{1}{2r_w^2} I_T A^2 \omega_n^2 \sin^2 (\omega_n t)$$

$$+ \frac{1}{2r_w^2} k_t A^2 \cos^2 (\omega_n t) \tag{17}$$

5.2.   Process of discharging energy

After the BW mechanism leaves the inclined plane, it begins moving on the horizontal plane, reaching a maximum distance ($x_{\max}$), until it arrives at P_3. At this point, the elastic band untwists; therefore, the device moves back and forward repeatedly, performing some cycles of a damped harmonic oscillator movement until stopping completely. If the movement is along the x-axis, and assuming there are no external forces, the balance of forces for damped harmonic oscillators is then [25]

$$-kx - c\dot{x} = m_T \ddot{x} \quad \rightarrow \quad \ddot{x} + \frac{c}{m_T}\dot{x} + \frac{k}{m_T}x = 0 \tag{18}$$

where the natural frequency (ω_n) and the damping ratio (ζ) are given by

$$\omega_n = \sqrt{\frac{k}{m_T}}, \quad \zeta = \frac{c}{2\sqrt{m_T k}} \tag{19}$$

Eq. (18) can be rewritten as [26]

$$\ddot{x} + 2\zeta\omega_n\dot{x} + \omega_n^2 x = 0 \tag{20}$$

A solution of Eq. (20) is assumed to be of the form $x(t) = Ae^{i\omega_n t}$, and using the quadratic formula $\alpha = -\zeta\omega_n \pm i\omega_n \sqrt{1 - \zeta^2}$, it takes the form [27]

$$x(t) = A_1 e^{(-\zeta\omega_n \pm i\omega_n \sqrt{1-\zeta^2})t}$$

$$+ A_2 e^{(-\zeta\omega_n \pm i\omega_n \sqrt{1-\zeta^2})t} \tag{21}$$

For $\zeta < 1$ (or $b/2m < \sqrt{k/m_T}$), the imaginary term in the exponent will be real and defined by the frequency of damped vibration $\omega_d = \omega_n \sqrt{1 - \zeta^2}$. Equation (21) can be rewritten using Euler's identity as

$$x(t) = e^{-\zeta\omega_n t}[C_1 \cos (\omega_d)t + e^{-\zeta\omega_n t} + C_1 \sin (\omega_d)t] \tag{22}$$

An alternative form of the solution is developed using the trigonometric identity as

$$x(t) = Ae^{-\zeta\omega_n t} \cos (\omega_d t + \phi_d) \tag{23}$$

where

$$A = \sqrt{x_0^2 + \left(\frac{\dot{x} + \zeta\omega_n x_0}{\omega_d} \right)^2}, \qquad \omega_d = \omega_n \sqrt{1 - \zeta^2}$$

and

$$\phi_d = \tan^{-1}\left(\frac{\sqrt{1-\zeta^2}}{\zeta}\right).$$

Now, we consider a single-degree-of-freedom torsional system with a small viscous damper. The equation of motion can be derived as

$$I_0 \frac{d^2\theta}{dt^2} + b_t \frac{d\theta}{dt} + k_t\theta = 0 \tag{24}$$

The solution of Eq. (24) can be exactly found as in the case of linear vibrations. The frequency of damped vibration is given by the same expression as Eq. (18) where ω_n is the undamped natural frequency given by

$$\omega_n = \sqrt{\frac{k_t}{I_0}} \tag{25}$$

and the damping ration β is

$$\beta = \frac{b_t}{2\sqrt{I_0 k_t}} \tag{26}$$

Then, the expression for the angular movement is

$$\theta(t) = Ae^{-\beta\omega_n t}\cos(\omega_d t - \phi_d) \tag{27}$$

Where ω_d is the damped frequency. The total energy of the BW mechanism for the discharge process can be expressed as

$$E_T = \frac{1}{2}m_T\dot{x}^2 + \frac{1}{2}I_T\dot{\theta}^2 + \frac{1}{2}k_t\theta^2 \tag{28}$$

where

$$\dot{x} = -A\omega_d e^{-\zeta\omega_n t}\sin(\omega_d t + \phi_d)$$
$$- A\zeta\omega_n e^{-\zeta\omega_n t}\cos(\omega_d t + \phi_d)$$
$$\dot{\theta} = -A\omega_d e^{-\beta\omega_n t}\sin(\omega_d t + \phi_d)$$
$$- A\omega_n\beta e^{-\beta\omega_n t}\cos(\omega_d t - \phi_d)$$

6. Results and Discussion

To validate the mathematical approach, a it was built prototype of the BW mechanism with two compact discs joined by three wooden sticks. An elastic band joins both compact discs. Table I summarizes the characteristics of the prototype.

TABLE I. Characteristics of the BW mechanism.

Quantity	Components	Mass [kg]	Dimensions [cm]
1	Counterweight	0.055	$d_C = 6$; $L_C = 6.5$
2	Wheels	0.015	$d_w = 12$
3	Shafts	0.0016	$d_s = 0.5$; $L_s = 6.5$
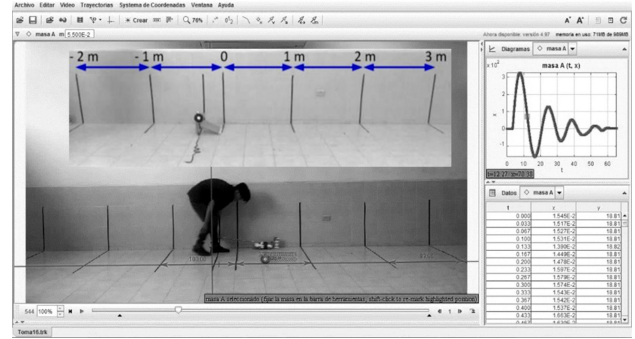
FIGURE 4. Displacement of BW mechanism with measurements.
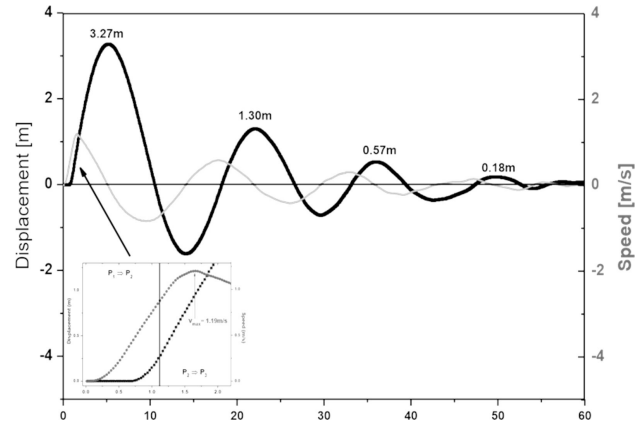
FIGURE 5. Displacement and speed of BW movement showing the zone of the charging energy process.

The BW prototype was placed on an inclined plane with a brake. When the brake is removed from the device, it starts to roll without slipping along the inclined surface with an angular speed. To obtain the experimental data, we used Tracker software, which is a free video analysis and modeling tool. The video was recorded with the camera of a typical smartphone, as shown in Fig. 4.

As can be seen from Fig. 5, the displacement is divided into two parts: the charging and discharging processes. In the charging process, the BW mechanism goes from P_1 to P_2; its maximum speed v_{max} is achieved at P_2, where v_{max} is approximately 1.19 m/s.

At the point P_3, the speed is $V = 0$ m/s. Using the data obtained with Tracker and Eq. (1)-(2), the potential energy is approximately 0.15 J, and the value decreases until reaching zero, as shown in Fig. 6.

This decrease is the result of the change in height from P_1 to P_2 in the inclined plane. The figure also shows that potential energy tends to increase slightly from zero when the BW mechanism moves from P_2 to P_3. Moreover, the figure shows that there is a contribution to the potential energy of the elastic band when the BW mechanism leaves the ramp. This contribution also can be seen in the total energy.

As the BW goes from P_1 to P_2, its kinetic energy tends to increase, because of an increase in speed while the BW mechanism is descending on the inclined plane. However,

when
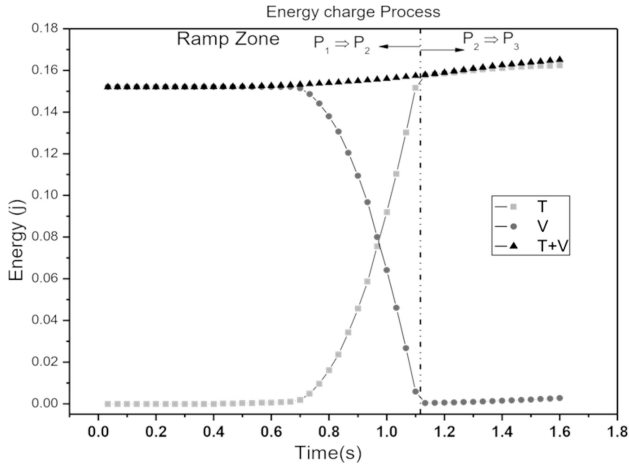
FIGURE 6. Behaviour of potential and kinetic energy during the charging process.
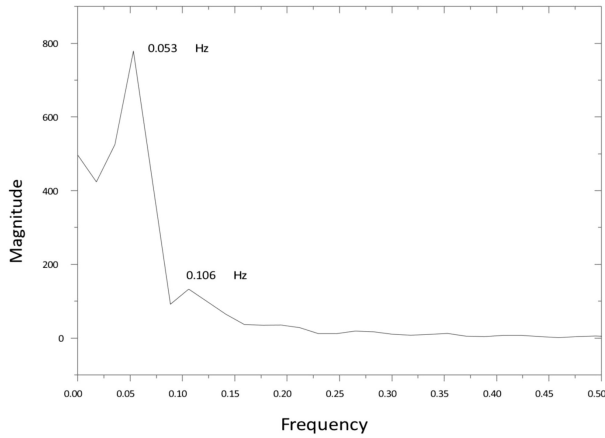
FIGURE 7. Graph of FFT applied to BW mechanism data.

the BW mechanism goes from P_2 to P_3, the kinetic energy also increases slightly, so the total energy tends to increase above even the potential energy. In the same way, this can be attributed to elastic kinetic energy, as shown in Fig. 6.

For the discharge process, the BW mechanism presents harmonic oscillations with almost three cycles. The amplitude of the oscillation decreases with time, and the viscous damping force dissipates. Because no work is being done on the system, this leads to a continual decrease in the potential and kinetic energy until it reaches equilibrium, as shown in Fig. 6. The vibrations of the BW mechanism are cyclic but not periodic. The logarithmic decrease is determined using the point $x_1 = x(t)$ and a point in a period after as $x_2 = (t + (2\pi/\omega_d))$, $x_1 = 3.27$ m, and $x_2 = 1.30$ m. The exponential decay is $\beta\omega_n t = 0.922$, with the damping ratio as $\beta = 0.152$.

Applying a fast Fourier transform (FFT) to the BW displacement, we show that there are two distinct frequency peaks, which turn out to be multiples of 0.053 Hz, as shown in Fig. 7. The angular frequency of damped vibration ω_d

is approximately 0.333 rad/s, and the undamped natural frequency is approximately 0.337 rad/s. Therefore, using the
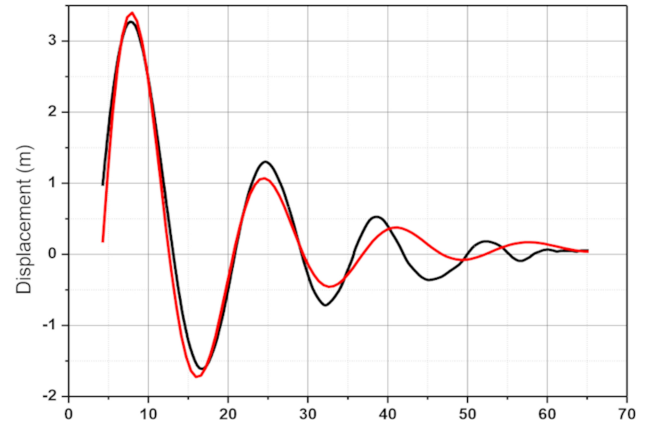
FIGURE 8. Experimental fit from BW displacement, using Eq. (23). Values are: $\zeta = 0.189$, $\omega_n = 0.37$ rad/s; $A = 5.65$ m and $x_0 = 0.12$ m (initial displacement).
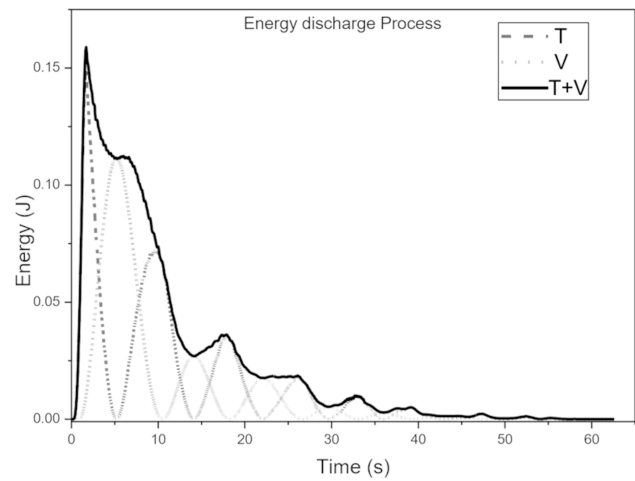
FIGURE 9. Graph of the energies present during movement.

initial conditions $x_0 = 0$, $\phi_d = (n\pi/2)$ and $A = (\dot{x}_0/\omega_d)$ in Eq. (23), we obtain the expression of displacement in the discharge process $x(t) = 3.6e^{-0.051t}\sin(0.33t)$. When comparing this expression with the values obtained experimentally, the experimental expression of displacement is $x(t) = 0.12 + 5.65e^{-0.07t}\sin(0.37t)$.

Plotting both expressions (Fig. 8), it is clear that there is an only slight difference in the first two cycles. However, in the following cycles, the graph shows notable differences. The variability in the expressions occurs because neither frictional forces nor the misalignment of the floor was not considered in the analysis.

In Fig. 9, we can observe the different changes between kinetic energy T and elastic potential energy V during the cyclic charge and discharge, which indicate the capacity of the elastic system to save energy and release it slowly between each cycle. The total energy of the system is strongly related to the cycles of the elastic potential energy, so that it acts like a rechargeable battery. At the end of each cycle,

the energy stored in the elastic element is transformed into translational and rotational kinetic energy. However, in each cycle, the BW mechanism shifts a shorter distance to the previous cycle; as a result, the storage and discharge of energy decrease.

7. Conclusion

This work shows students that this system has to be divided into two scenarios for its analysis: when the mechanism rolls on the inclined plane (energy charge process), and when it rolls on a horizontal surface (energy discharge process). The derived equations demonstrate satisfactory results. However, in the energy discharge process, there is a difference after the first two cycles, because neither frictional forces nor, the misalignment of the floor was considered in the analysis. Besides, the potential and kinetic energy depend on the torsion of the elastic band, as it stores and releases the energy of mechanical. A complete study of the frictional forces is suggested to complete the mathematical approach. In relation to students, we observed that one of the major problems in this analysis was the construction of Free-Body diagram, due to the system has multiple components. Therefore, it is suggested to reinforce the construction free body diagram of 3D objects in the classroom.

List of Symbols

Greek letters

α	Phase angle (rad)
ζ	Damping ratio (cycles/s)
θ	Rotation angle (rad)
$\dot{\theta}$	Angular velocity (rad/s)
$\ddot{\theta}$	Angular acceleration (rad/s^2)
ϕ	Angle of inclined plane (grades)
λ	Lagrange multiplier
ω	Angular frequency (rad/s)
ω_d	Frequency of damped vibration (rad/s)
ω_n	Natural Frequency (rad/s)

Nomenclature

A	Amplitude (maximum value)
c	Viscous damping coefficient (N s /m)
C	Constant of integration
d	Diameter (m)
e	Eulers identity
E	Energy (J)
g	Gravity (m/s^2)
i	Imaginary part
I	Moment of inertia (kgm^2)
k	Spring stiffness (N/m)
k_t	Torsional stiffness (lbft/rad)

l	Lenght of ramp (m)
L	Length (m)
$\mathbf{L}$	Lagrangian function
m	Mass (kg)
P	Position
r	Radius (m)
t	Time (s)
T	Kinematic energy (J)
V	Potential energy (J)
x	Position in the horizontal plane (m)
$\dot{x}$	Velocity in x (m/s)
$\ddot{x}$	Acceleration in x (m/s^2)
y	Position in the vertical plane (m)
$\dot{y}$	Velocity in y (m/s)
$\ddot{y}$	Acceleration in y (m/s^2)

Subscripts

C	Counterweight
d	Damped vibration
G	Center of mass
n	Natural
p	Periphery
s	Shaft
sp	Elastic band
T	Total
w	Wheel

1. Z. B. Takaoglu, *Universal Journal of Educational Research* **6.4** (2018) 653-660.

2. U. İYİBİL. *Journal of Educational Science* (2011) 1-8.

3. E. Tatar and M. Oktay. *Int J Environ Sci Te Journal* **2.3** (2007) 79-81.

4. V. A. Heuvelen, and X. Zou, *Am. J. Phys* **69.2** (2001) 184-194.

5. A. Tiberghien, *Research in science education in Europe* (1996) 100-114.

6. Liu, Xiufeng *et al.*, *Journal of Research in Science Teaching: The Official Journal of the National Association for Research in Science Teaching* **39.5** (2002) 423–441.

7. G. Barceló, *Journal of Applied Mathematics and Physics* **2.07** (2014) 569.

8. F. Hess, *SCI AM* **219.5** (1968) 124.

9. A. Azuma *et al.*, *J. Guid. Control Dyn.* **27.4** (2004) 545.

10. T. E. Montroy *et al.*, *ApJ* **647.2** (2006) 813.

11. Ehsani Mehrdad *et al., Modern electric, hybrid electric, and fuel cell vehicles*, 3rd ed. (CRC press2018), pp. 6 (2018).

12. Y. Yavin and C. Frangos, *Math. Comput. Model.* **20** (1994) 81.

13. Y. Yavin and C. Frangos, *Comput. Methods Appl. Mech. Eng.* **127** (1995) 227.

14. P. D. Kemp and Y. Yavin, *Comput. Math. Appl.* **39** (2000) 237.

15. R. H. Cushman and J. J. Duistermaat, *Regul. Chaotic Dyn* **11** (2000) 31.

16. De Ambrosis, Anna, *et al.*, *Eur. Phys. J* **36** (2015) 1.

17. D. P. Maloney, *Journal of Research in Science Teaching* **22**, (1985), 261.

18. M. Batista, *Int J Non. Linear Mech.* **41** (2006) 850.

19. M. Batista Milan, *Regul. Chaotic Dyn.* **13** (2008) 344.

20. T. Soldovieri, *Introducción a la mecánica la Lagrange y Hamilton*, 2nd ed. (Universidad del Zulia. Preprint, 2010), pp. 42-74.

21. M. Zefran, Milos and B. Francesco, *Robotics and Automation Handbook* (2005) 5.

22. D. Hestenes, *New foundations for classical mechanics*. 1st ed. (Springer Science & Business Media, 2012) pp. 419-501.

23. V. I. Arnold, *Mathematical methods of classical mechanics*, 2nd (New York: Springer Science & Business Media, 2013), pp. 53-154.

24. E. T. Whittaker, *A treatise on the analytical dynamics of particles and rigid bodies*, 4th ed. (Cambridge University Press, 1988), pp. 26-50.

25. H. Goldstein, *et al*, *Classical mechanics*. 3rd ed. (Addison Wesley, 2002), pp. 1-81.

26. S. S. Rao and F. F. Yap, *Mechanical vibrations*, 5th ed. (Upper Saddle River: Prentice hall, 2011), pp. 4-237.

27. M. Géradin and D. J. Rixen, *Mechanical vibrations: theory and application to structural dynamics*, 3rd ed. (John Wiley & Sons, 2014,) pp. 137-204.